Revista Brasileira de Recursos Hídricos
Brazilian Journal of Water Resources
Versão On-line ISSN 2318-0331
RBRH, Porto Alegre, v. 27, e19, 2022
Scientific/Technical Article

https://doi.org/10.1590/2318-0331.272220220017

Hydrological risk of dam failure under climate change

Risco hidrológico de falha da barragem sob mudanças climáticas

Brenda Lara Duarte Souza Carneiro[1], Francisco de Assis de Souza Filho[1], Taís Maria Nunes Carvalho[1] & João Batista Sousa Raulino[1]

[1]Universidade Federal do Ceará, Fortaleza, CE, Brasil

E-mails: brenda_carneiro@hotmail.com (BLDSC), assis@ufc.br (FASF), taismarianc@gmail.com (TMNC), jbraulinos@gmail.com (JBSR)

Received: March 04, 2022 - Revised: May 25, 2022 - Accepted: June 29, 2022

ABSTRACT

Most water infrastructure was designed for climate conditions and demands that have been rapidly changing. In this study, we investigate flood magnitude and dam safety under climate change, using an ensemble of CMIP6 climate models, coupled to a hydrological model. We compare historical and future climate conditions of a watershed in Ceará, Northeast Brazil. Climate models revealed a wide range of risk levels of flood and hydrological failure. Half of the climate scenarios indicated a reduction in the flood return period. A flood associated with a 1000-year storm had an occurrence probability about 12 times higher when comparing the SSP5 8.5 scenario with historical conditions. In one more critical scenario, the water depth exceeded the height of the dam's crest. When considering a flood associated with a decamillennial storm, dam collapse risk was increased. Climate change might increase the risk of water infrastructure failure, which needs to be adapted to ensure the safety of the water system stakeholders.

Keywords: Climate change; Extreme events; Intensity-duration-frequency; Risk assessment; Dam safety.

RESUMO

A maior parte das infraestruturas hídricas foram projetadas para condições climáticas e demandas que estão mudando rapidamente. Neste estudo, foi investigada a magnitude das inundações e a segurança de barragens em cenários de mudanças climáticas, utilizando um conjunto de modelos climáticos do CMIP6, acoplados a um modelo hidrológico. Foram comparadas as condições climáticas históricas e futuras de uma bacia hidrográfica do Ceará, Nordeste do Brasil. Os modelos revelaram uma ampla gama de níveis de risco de inundação e falha hidrológica. Metade dos cenários climáticos indicaram uma redução no período de retorno das cheias. Uma inundação associada a uma chuva de 1000 anos teve sua probabilidade de ocorrência cerca de 12 vezes maior, quando comparado o cenário SSP5 8.5 com as condições históricas. No cenário mais críticos, a lâmina d'água ultrapassou a altura da crista da barragem. Ao considerar a cheia associada a uma chuva decamilenar, o risco de colapso da barragem foi aumentado. As mudanças climáticas podem aumentar o risco de falha da infraestrutura hidráulica, que precisa ser adaptada para garantir a segurança das partes interessadas do sistema hídrico.

Palavras-chave: Mudanças climáticas; Eventos extremos; Intensidade-duração-frequência; Avaliação do risco; Segurança de barragens.

INTRODUCTION

The warming of the climate system, highly associated with global changes in the magnitude and frequency of precipitation events (Kuo & Gan, 2015; Orlowsky & Seneviratne, 2012) can have serious impacts on water resources management. Although the response of flood magnitudes to precipitation extremes is not entirely clear and climate models have high uncertainties associated with them (Brunner et al., 2021), several studies have indicated an increasing trend of vulnerability to floods in urban systems and reservoirs (Kuo & Gan, 2015; Lin et al., 2021; Maurer et al., 2018).

Globally, most of the existing dams were built with less restrictive design criteria than today's (Tofiq & Güven; 2015), and now require a reexamination of flood planning strategies. There has been an increasing interest in analyzing the impact of climate changes in dam flood design, mostly by comparing future projections with historical data (Kuo & Gan, 2015; Maurer et al., 2018; Tofiq & Güven, 2015).

In low-latitude regions, such as the Brazilian northeast, total rainfall events tend to decrease in volume and increase in intensity in the next century (Medeiros de Saboia et al., 2020). The semiarid, which accounts for about 60% of the region, has a unique river regime and is frequently affected by droughts. In Ceará, several surface reservoirs have been built to guarantee water supply, especially during the "hydraulic phase" (1877-1950), when public policies mainly focused on building hydraulic infrastructure (Campos, 2015). Currently, 155 reservoirs are considered strategic for the state, as these account for most of the pluriannual storage capacity (18.63 billion m^3) and are spread over its 12 hydrographic basins.

Although national committees and guidelines on dam inspection have been created in the 1930s, it was not until the 2010s that a national policy for dam security was implemented in Brazil. In Ceará, an ordinance law establishing the requirements for dam inspection was published in 2017. As most of the strategic dams were dimensioned for historical climate conditions, climate change can have severe consequences for dam security and increase their risk of failure (Ho et al., 2017; Lee & You, 2013; Mallakpour et al., 2019). Hence, climate risk must be considered when elaborating safety plans so that stakeholders can take proactive efforts to prevent dam failure and facilitate response actions.

Many researchers have addressed the impact of future climate on dam safety in the United States (Ho et al., 2017; Lin et al., 2021; Mallakpour et al., 2019; Maurer et al., 2018), Europe (Brunner et al., 2021; Willems, 2013), and Asia (Lee & You, 2013; Tofiq & Güven, 2015), but little effort has been put to analyze the effects of climate change on flood magnitude in the Global South or in semiarid regions. To date, few studies have combined IDF curve ensembles of CMPI6 models with hydrological modeling to obtain the risk of hydrological failure of dams. This approach can be useful for risk assessment and for informing decision-makers on dam protection. The update of IDF curves (commonly used for infrastructure design (Ragno et al., 2018)) can also be crucial for analyzing climate change effects on water infrastructure and supply (Simonovic et al., 2017).

The main purpose of this study is to analyze the safety of a strategic dam of Ceará, Brazil for historical (1948-2019) and future climate scenarios (2020-2100). The IDFs of the basin were updated for an ensemble of climate models and were coupled to a hydrological model. We assess the risk of hydrological failure of the dam by comparing the average recurrence time for historical and projected floods. This approach is advantageous because it can be easily replicated to analyze the risks associated with future climate in other regions of the world. As the uncertainties associated with the effects of climate extremes can be site-specific, such a reproducible methodology can be very informative and useful for water resources planning.

DATA AND METHODS

The methodological strategy adopted in this study can be summarized as follows (Figure 1): (i) obtain historical (rain-gauge stations) and future (projected with GCMs) maximum daily rainfall data; (ii) adjust the data for future climate scenarios using statistical downscaling with the equidistance quantile matching method (EQMM) (Srivastav et al., 2014); (iii) generate the IDFs for the baseline and future climate scenarios; (iv) simulate extreme rainfall events using hydrological modeling with the HEC-HMS model and calculate the overflow of the hydraulic structures; (v) calculate the average recurrence interval of the extreme rainfall event and the probabilities of structure collapse for each scenario.

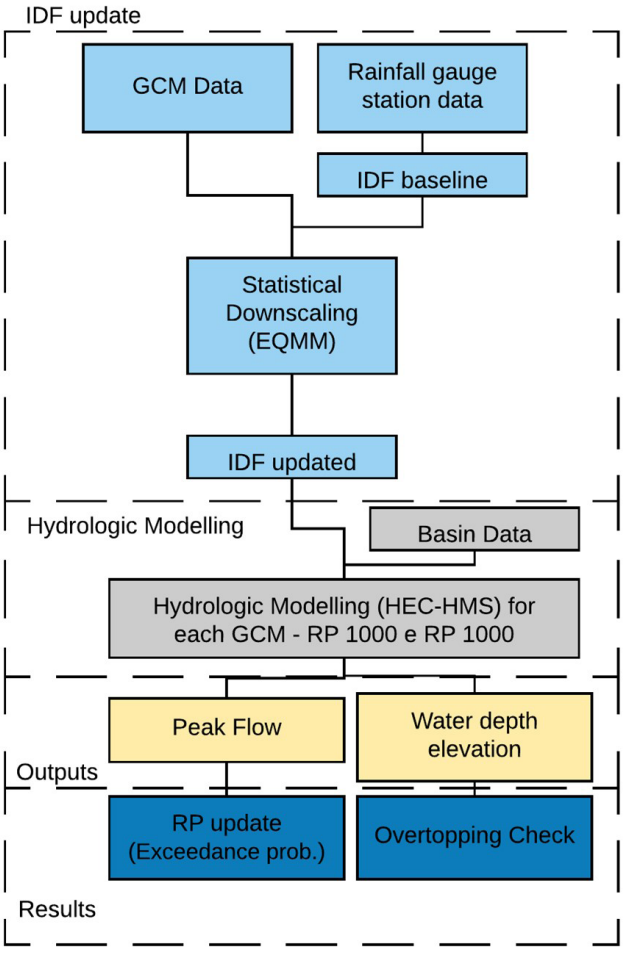

Figure 1. Flowchart of the methodology applied in the study.

Study area

The Araras reservoir is located in the Acaraú basin, in Ceará, Brazil (Figure 2). The reservoir is the fourth largest in the state, with a capacity of 891 hm^3 and a catchment area of 3517 km2. The dam was built in 1958 to control the floods of the Acaraú River and mitigate the flood risk in the downstream community; currently, it supplies five municipalities of the region and is also used for irrigation and hydropower generation (Companhia de Gestão dos Recursos Hídricos, 2010). The Acaraú basin is a low-latitude region, with a warm, semi-arid tropical climate, an elevation of 115 to 1,124 m above sea level, and an average annual rainfall of 878 mm. The basin is divided into five subbasins (Table 1).

Precipitation data

Historical precipitation data (1948-2019) was obtained from five rain-gauge stations (Figure 2). Future precipitation data (2020-2100) from four GCMs models (Table 2) and emission scenarios SSP2 4.5 and SSP5 8.5 were obtained from the Coupled Model Intercomparison Project Phase 6 (CMIP6) (Eyring et al., 2016). Figure 3 presents the distribution of the GCMs precipitation data. The models from CMPI6 should form the basis of climate projections in the IPCC's sixth assessment report. The emissions scenarios SSP2 4.5 and SSP5 8.5 are similar to RCPs 4.5 and 8.5 (Hausfather & Peters, 2020), but with different emissions paths and mixes of CO2 and non-CO2. While in SSP2 4.5 it is assumed that the carbon dioxide emission levels will be maintained, SSP5 8.5 is a pessimistic scenario, in which carbon dioxide emission levels are assumed to increase drastically.

Many models are available from CMIP6, leading to divergent climate projections and a certain degree of uncertainty in risk analysis. We chose four of these models to represent the variability among them. The climate models we selected for this study were based on a previous study on water availability uncertainty under climate change, which analyzed some of the CMIP6 models for Ceará (Estácio, 2020). We must emphasize that this can be a significant source of uncertainty in climate risk assessment, as

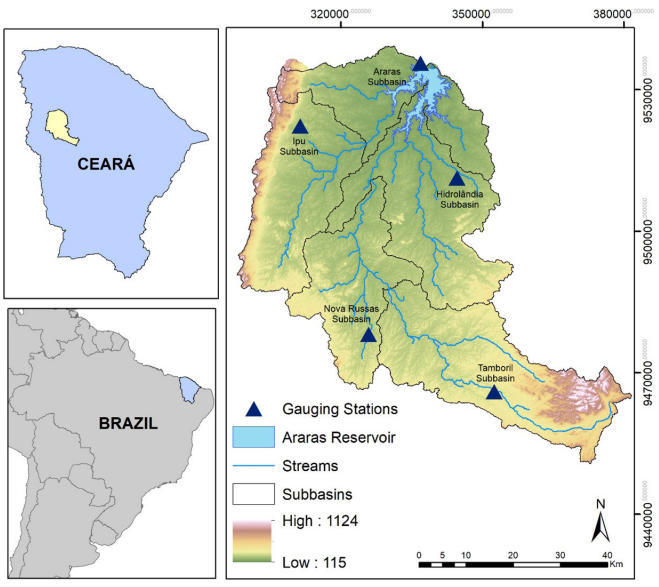

Figure 2. Location of the Araras Reservoir in the State of Ceará, Brazil.

Table 1. Characteristics of the subbasins of the Araras reservoir basin.

Subbasin	Area (km^2)	River Length (km)	Time of concentration (min)
Araras	546.49	20.28	541.90
Ipu	679.52	42.84	509.47
Hidrolândia	796.54	29.54	636.75
Nova Russas	622.97	31.95	863.46
Tamboril	842.48	82.33	511.20

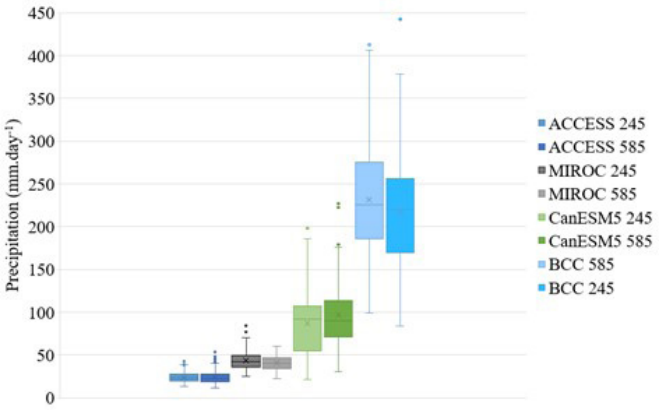

Figure 3. Distribution of the maximum annual daily precipitation data extracted from the GCMs ACCESS-ESMI1-5, BCC-CSM2-MR, CanESM5, and MIROC-ES2L, for the scenarios SSP2 4.5 (245) and SSP5 8.5 (585).

Table 2. GCMs used in this study.

Model CMIP6	Research Center	Country	Spatial Resolution	Nominal Resolution
ACCESS-ESMI1-5	Centre for Australian Weather and Climate Research	Australia	1.9°x1.3°	250km
BCC-CSM2-MR	Beijing Climate Center	China	1.1°x1.1°	100 km
CanESM5	Canadian Centre for Climate Modelling and Analysis	Canada	2.8°x2.8°	500km
MIROC-ES2L	Japan Agency for Marine-Earth Science and Technology	Japan	2.8°x2.8°	500km

these models make different assumptions on the global climate system. However, they still provide a range of the risk associated with climate change and the magnitude of future precipitation events. Model choice could be biased (if the selection includes only a certain trend in precipitation change), hence one must be careful when analyzing the results of climate assessment.

Statistical downscaling and spatial data interpolation

GCMs provide climate information for a coarse spatial resolution that usually needs to be transformed to a smaller scale, so the data can be used to assess regional climate conditions. Downscaling approaches can be broadly classified as either dynamic or statistical. Statistical downscaling procedures are based on transfer functions which relate the GCM models with the local historical data (Srivastav et al., 2014).

In this study, downscaling was performed using EQMM (Srivastav et al., 2014), to correct the statistical bias present in the samples generated by the GCMs (Saboia et al., 2020). In this method, the quantiles cover the distribution of the data and the coefficients of the linear quantile function to capture the biases (distance or error) between the GCM output and historical observed data (Schardong et al., 2021).

The EQMM methodology combines two processes: (i) spatial downscaling; relating the maximum annual precipitation values and the precipitation observed in the baseline period; (ii) temporal downscaling; relating the historical and future annual maximum rainfall outputs from GCMs (bias correction) (Srivastav et al., 2014).

It is necessary to investigate non-stationarity in historic data, the methodology adopted for the development of non-stationary IDFs includes: (i) Statistical analysis for fitting Generalized Extreme Value (GEV) distribution using the Maximum Likelihood method; (ii) Statistical analysis (corrected Akaike Information Criteria - AICc) for identifying non-stationarity and defining the most suitable model; and assessing the statistical significance of the non-stationary model in comparison to the stationary model; and (iii) IDF updating algorithms to address the impacts of climate change for gauged locations (Silva & Simonovic, 2020). Statistical significance was checked using the Likelihood ratio test, through which the negative log-likelihood of two models is compared to test the null hypothesis that there is no trend in a parameter.Then, a statistical relationship was established between the maximum annual precipitation data for 1934-2014 extracted from the GCMs and rain-gauge stations. A probabilistic adjustment was established between the future forecasts and the climate model's base period.

GCM data must be spatially interpolated to the rain-gauge station coordinates to assimilate the variations in the distribution between these models and the observed historical series (Schardong et al., 2021). Precipitation data were interpolated using the inverse square distance weighting method, which was applied with the IDF CC tool (Schardong et al., 2021).

IDF curves estimation

As the region lacks a pluviograph, the Isozones method (Torrico, 1974) was used to disaggregate daily rainfall data into sub-daily data and estimate the IDF curves. This method correlates data from pluviometric and pluviographic stations to extract the relationship between the 1h/6 min and 24h rainfall for homologous areas (isozones), which is constant for the same average recurrence interval (ARI) and does not depend on the precipitation level. Hence, each isozone is associated to disaggregation coefficients for different ARIs (Torrico, 1974).

For each rain-gauge station, the annual maximum daily precipitation (AMDP) series were fitted to a probabilistic distribution. The AMDP data are fitted using extreme value distributions like Gumbel, Generalized Extreme Value (GEV), Log-Pearson, Log-Normal, among others (Silva & Simonovic, 2020). The maximum daily precipitation was obtained for ARIs of 1000 and 10000 years. Then, the precipitation of 24h was disaggregated into 6-, 60-, and 1440-min intervals using the coefficients of the corresponding isozone, which were used to estimate the IDF curves.

Hydrological modeling

Hydrological modeling of the basin was performed using the HEC-HMS software, where it is possible to simulate rainfall-runoff processes in catchments, which can be composed by a group of interconnected subbasins (Campos, 2009).

Nine scenarios were simulated: one scenario corresponding to the historical precipitation data (baseline) and eight scenarios corresponding to the combination of the four GCMs and two SSPs. Design rainfall was calculated with the updated IDF equations, considering ARIs of 1000 and 10000 years, which are usually recommended for dimensioning dam spillways (Chow, 2010; Franco, 2014; Villela & Mattos, 1975). The extreme rainfall duration was calculated using the Kirpich equation, according to the time of concentration of each subbasin. The hyetograph for each scenario was calculated using the alternating block method (Chow, 2010).

Finally, hydrographs for each scenario were obtained using the Curve Number (CN) method of the Soil Conservation Service (SCS). The SCS method requires basin parameters (such as area, perimeter, length, and slope of the basin), precipitation data, and the CN value, that depends on the soil and land cover conditions of the basin (United States Department of Agriculture, 1986). The CN values for the Araras reservoir basin were estimated as recommended by Luna (2000).

Risk assessment

To assess the risk of failure associated with climate change, two criteria were determined: (i) the probability of occurrence of flood events, and (ii) the impact of the risk (severity). One should note that a 1000-year (10000-year) storm is not the same as a 1000-year (10000-year) flood. Here, we analyze the effect of future changes in precipitation intensity on flood risk. We defined the risk of collapse as the occurrence of a flood with a peak flow

greater than the system's capacity, which we assumed to be the peak flow obtained for the baseline scenario (*Qobs*). Hence, the risk of failure is the exceedance probability of $Q_i > Qobs$, as follows:

$$C = P[Q_i > Qobs] \quad (1)$$

where Q_i is the peak flow obtained for future climate scenarios. The severity of the events for which the baseline peak flow was exceeded was addressed with the risk of overtopping. Overtopping is mainly caused by insufficient flood storage or inadequate spillway capacity and can be identified when the water level is above the dam crest after a flood has been regulated (Lee & You, 2013). Here, we assume the dam has failed when the water elevation exceeds the dam crest elevation (156.4 m).

RESULTS AND DISCUSSION

Updated IDF curves

Figure 4 presents the updated IDF curves for all climate models and scenarios, for the five subbasins analyzed in this study. These curves were calculated for an ARI of 1000 years. The BCC-CSM2-MR and ACCESS-ESMI1 models provide the most significant changes in the relationship between precipitation and time of concentration in all basins analyzed here. The CanESM5 and MIROC-ES2L models resulted in little variation in the IDF curves; these two have the lowest spatial resolutions of the analyzed models (approximately 2.8°x2.8°).

We have also analyzed the percent variation of the total precipitation in the basins for a future climate in comparison to the baseline (historical climate) scenario. Total precipitation was calculated using the IDFs previously calculated and the time of concentration calculated for each subbasin (Table 3).

ACCESS-ESMI1, with a spatial resolution of about 1.9°x1.3°, had the highest percent variation among the models (132%). The model indicated the most intense precipitation events of the scenario SSP5 8.5, with an average percent variation of 71.5% and the had high variance among the variation in precipitations, with values ranging between -5.5% (SSP2 4.5) and 132% (SSP5 8.5).

The BCC-CSM2-MR model, which has the best spatial resolution (approximately 1.1°x1.1°), indicated a possible increase in precipitation for both emission scenarios. Interestingly, SSP5 8.5 was the one with the largest increase (about 16.4%).

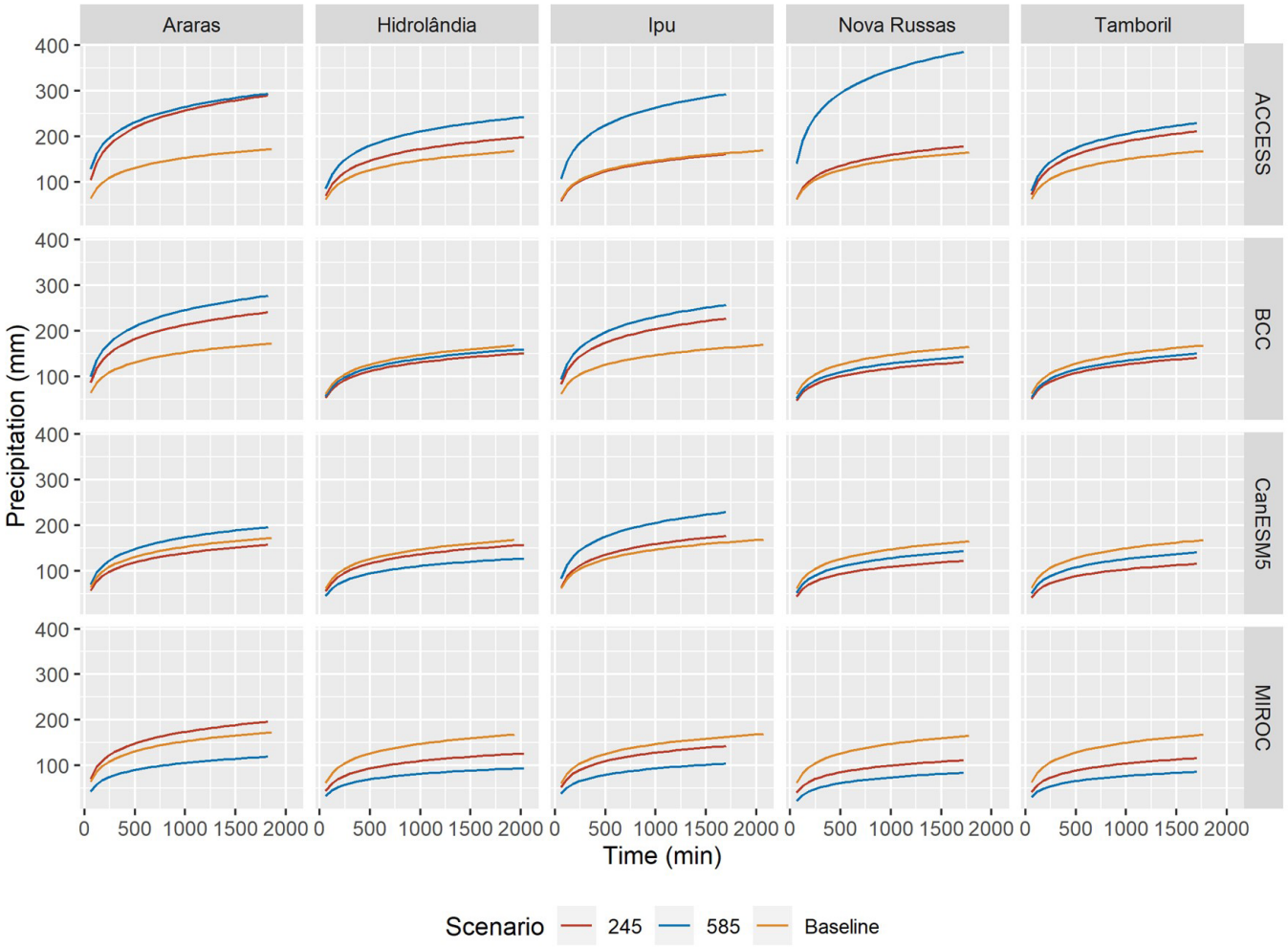

Figure 4. Updated precipitation curves (ARI = 1000 years) for all subbasins and the eight scenarios of climate change, i.e., the combination of four GCMs and the two scenarios SSP2 4.5 (245) and SSP5 8.5 (585).

The CanESM5 model presented high variance among the percent variation of precipitation in the basins, indicating, on average, reduced precipitation for the scenario SSP2 4.5 and almost no change for scenario SSP5 8.5. The MIROC-ES2L model also had high reduced precipitation for both scenarios, SSP2 4.5 (about -18.3%) and SSP5 8.5 (about -42.8%), indicating driest future scenarios.

Hydrological modeling under climate change

Hydrological simulations of an extreme rainfall event were performed for each climate change scenario, considering an ARI of 1000 years (Figure 5) and 10000 years (Figure 6). For each simulation, we extracted the values of the peak effluent flow and the water depth on the spillway. Then, we compared the effects of the millenary and the floods associated with decamillennial storms to the baseline scenario by evaluating the percent variation between each of these variables.

The flood associated with a millenary storm was overcome in half of the scenarios, with the most extreme percent variation for the scenario ACCESS/SSP5 8.5, which had an increase in peak flow of about 109.4%.

We assumed that dam overtopping happens when the water elevation in the spillway is higher than the elevation of the dam

Table 3. Average variation of the total precipitation in the subbasins for each climate change scenario in comparison to the baseline scenario. The highest percentage variations for each scenario are highlighted in bold.

Model	Scenario	Subbasins					Mean
		Araras	Ipú	Hidrolândia	Nova Russas	Tamboril	
ACCESS	SSP2 4.5	**67.7%**	-5.5%	16.7%	7.1%	25.3%	22.3%
	SSP5 8.5	74.2%	72.1%	42.7%	**132%**	36.4%	71.5%
BCC	SSP2 4.5	**39.2%**	33.5%	-11.2%	-20.8%	-15.8%	5.0%
	SSP5 8.5	**60.3%**	51.1%	-5.7%	-13.5%	-10.2%	16.4%
CanESM5	SSP2 4.5	-9.0%	4.2%	-7.4%	-26.4%	**-30.9%**	13.9%
	SSP5 8.5	13.6%	**34.6%**	-24.8%	-13.7%	-15.8%	-1.2%
MIROC	SSP2 4.5	13.4%	16.1%	-25.5%	**-32.8%**	-30.6%	18.3%
	SSP5 8.5	31.0%	38.8%	-44.6%	**-50.9%**	-48.6%	42.8%

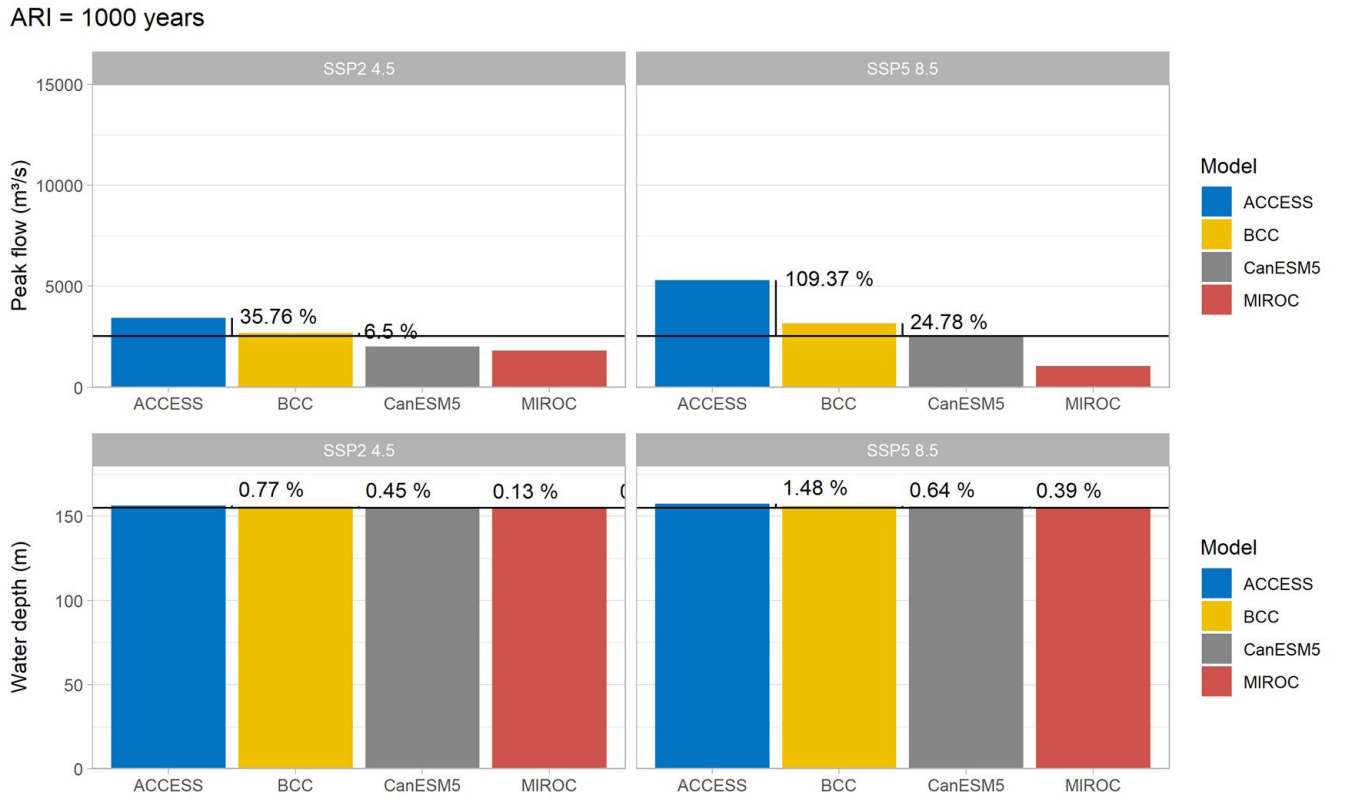

Figure 5. Peak flow and water depth values for each climate change model and emission scenario, for an ARI of 1000 years. The solid black line represents the value for the baseline (historical) scenario. The vertical solid lines at the right side of the bars represent the percent variation between the baseline and the corresponding scenario; this line was included only for the models which presented values of peak flow and water depth higher than the baseline.

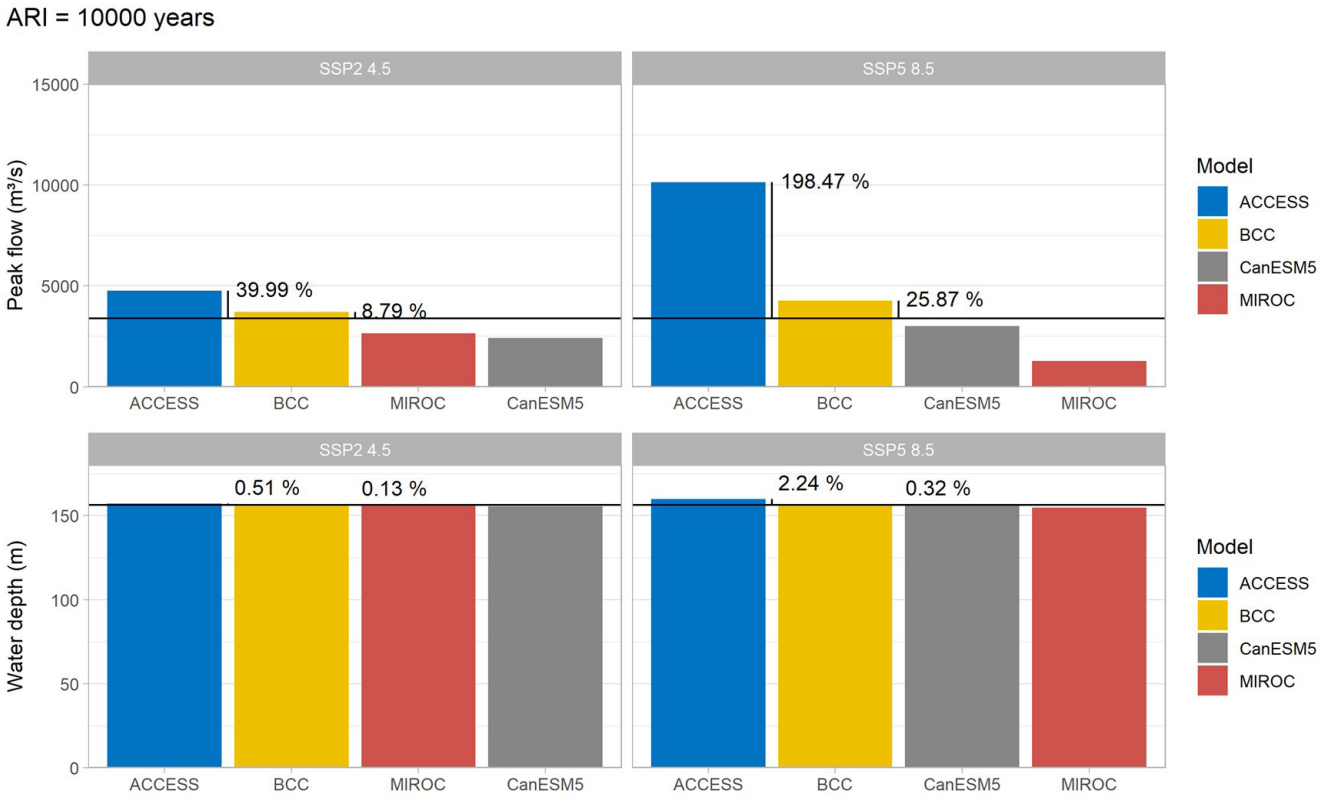

Figure 6. Peak flow and water depth values for each climate change model and emission scenario, for an ARI of 10000 years. The solid black line represents the value for the baseline (historical) scenario. The vertical solid lines at the right side of the bars represent the percent variation between the baseline and the corresponding scenario; this line was included only for the models which presented values of peak flow and water depth higher than the baseline.

crest (156.4 m). This situation, which might result in the collapse of the structure, happened in one scenarios: the ACCESS/SSP5 8.5.

When considering a rarer extreme rainfall event, i.e., an ARI of 10000 years, flood magnitudes were increased in comparison to the millennial event. The flood magnitude of the baseline scenario was exceeded in half of the scenarios. Overtopping was also observed in four scenarios. The CanESM5 and MIROC models indicated a decrease in peak flows for both extreme events/ARIs considered.

Other studies show the effects of climate change on extreme flood events, Kuo & Gan (2015) analyzed the risks of exceeding an intensive storm in the face of climate changes in an urban drainage system and found an increasing trend of vulnerability to floods. A project previously dimensioned with a 50-year project life would have your risk increased by 9% and 1-hour storms duration, then a 50-year storm event has become more recurrent, like a 29-year event.

Maurer et al. (2018) estimated the frequency of future peak flows for the western United States. Based on climate projections for 421 sites throughout the study area, flood recurrence times were estimated for the current scenario and future projection scenarios. Using the most critical gas emission scenario, an increase in peak flows was observed, reaching up to 43% of the increase in expected flows by the end of the 21st century. In terms of the flood return period, extreme events of 40 years, had 2.5 more chances of occurring.

Frequency of extreme events

After simulating the rainfall event with an ARI for 1000 years using hydrological modeling, we calculated the new ARIs for each scenario (Table 4). This approach recalls the concept of "recurrence reduction", which was used in previous studies on flood risk assessment (Bartiko et al., 2017; Vogel et al., 2011). Recurrence reduction is the reduction in the ARI of future floods associated with a flood in some reference year (Vogel et al., 2011). Although the actual ARI of reference floods is not necessarily the same as the one of projected storms, we use the new ARIs as proxies of flood risk associated with changes in precipitation.

For the most critical scenario, ACCESS SSP5 8.5, the 1000-year average recurrence interval has been shortened to 82 years, a 12-fold increase in occurrence probability. For the BCC SSP5 8.5 scenario, the 1000-year average recurrence interval was reduced to 114 years, increasing the occurrence probability of the event by about 8.77 times. CanESM52 4.5 and MIROC SSP5 8.5 were the periods with the lowest precipitation; These models overestimated the ARIs, exceeding 10000 years.

The empirical cumulative distribution of the exceedance probabilities was calculated for the climate change scenarios analysed in this study. Figure 7 shows that the flood associated with a millenary storm has a 63.8% chance of being overcome.

Table 4. Updated ARI of the extreme precipitation event for each climate scenario.

Scenario	Model	ARI (years)
SSP2 4.5	ACCESS	204
	BCC	523
	CanESM5	-
	MIROC	7252
SSP5 8.5	ACCESS	82
	BCC	114
	CanESM5	1260
	MIROC	-

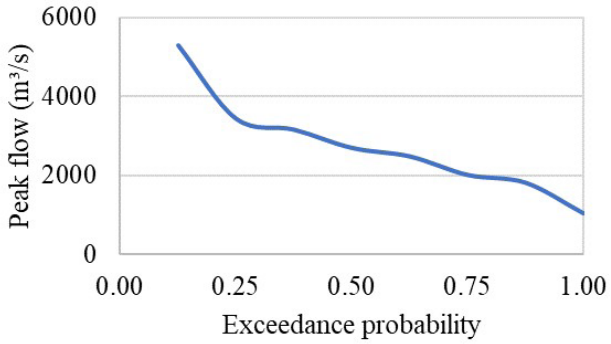

Figure 7. Current flood exceedance probabilities in a climate change scenario, for an ARI of 1000 years.

CONCLUSIONS

Using projections from GCMs and two emission scenarios, the IDFs of the Araras reservoir basin were updated and hydrological modelling was performed. The IDF curves generated for future climate indicated a large variance in precipitation levels, which is associated with the uncertainty and imprecision of global climate prediction models.

The flood magnitude associated with a millenary rainfall event was exceeded in half of the future climate scenarios when compared to the baseline scenario. The dam was overtopped in one scenario, with an ARI about 12 times lower. These results indicate an elevated occurrence probability of hydrological failure, which represents high risks for the downstream population and the increased need to ensure dam safety in a warmer climate.

When considering a rarer extreme event (with an ARI of 10000 years), peak flow magnitudes increased significantly, proving the greater damage caused by rarer events. The exceeding probability of the historical flood is about 64% for climate change scenarios, indicating that despite the uncertainties associated with climate projections, the risk of hydrological failure in the future can be worrisome. In this context, proposals of planning, projects, maintenance, and operation of infrastructure must address the possible effects of climate change.

Finally, we must emphasize that climate risk analysis includes several uncertainties associated with climate models, scenarios, sampling, and biases. In this study, only a few models of the CMIP6 database were considered. Second, although land use and occupation changes were not accounted for in this study, these can have a significant impact on flood risk and dam safety. Future studies on dam safety could include such effects by modelling the CN of the basins.

DATA AVAILABILITY STATEMENT

The GCM data of CMIP6 were extracted from the Earth System Grid Federation (ESDF) website (https://esgf-node.llnl.gov/projects/cmip6/). The rain-gauge measured rainfall series were obtained from the database of the National Water Agency (http://www.snirh.gov.br/hidroweb/).

ACKNOWLEDGEMENTS

The first author thanks the master's degree scholarship from the Brazilian National Council for Scientific and Technological Development (CNPq)

The third author thanks the doctor's scholarship from the National Council for the Improvement of Higher Education (CAPES)

The fourth author thanks the doctor's degree scholarship from the National Council for the Improvement of Higher Education (CAPES)

REFERENCES

Bartiko, D., Chaffe, P. L. B., & Bonumá, N. B. (2017). Não-estacionariedade em séries de vazões máximas diárias do Sul do Brasil. *Revista Brasileira de Recursos Hídricos*, *22*, e48, http://dx.doi.org/10.1590/2318-0331.0217170054.

Brunner, M. I., Swain, D. L., Wood, R. R., Willkofer, F., Done, J. M., Gilleland, E., & Ludwig, R. (2021). An extremeness threshold determines the regional response of floods to changes in rainfall extremes. *Communications Earth & Environment*, *2*(1), 173. http://dx.doi.org/10.1038/s43247-021-00248-x.

Campos, J. N. B. (2009). *Lições em modelos e simulação hidrológica* (166 p.). Fortaleza: ASTEF/Expressão Gráfica.

Campos, J. N. B. (2015). Paradigms and public policies on drought in Northeast Brazil: a historical perspective. *Environmental Management*, *55*(5), 1052-1063. PMid:25604214. http://dx.doi.org/10.1007/s00267-015-0444-x.

Chow, T. V. (2010). *Applied hydrology*. New York: Tata McGraw-Hill Education.

Companhia de Gestão dos Recursos Hídricos – COGERH. (2010). *Plano de gerenciamento das águas da bacia do Acaraú. Fase 2: planejamento.* Fortaleza: COGERH.

Estácio, Á. B. S. (2020). *Climate change and model parameter uncertainties propagated to ungauged reservoir catchments in Ceará: a study for water availability assessment*. Fortaleza: Universidade Federal do Ceará.

Eyring, V., Bony, S., Meehl, G. A., Senior, C. A., Stevens, B., Stouffer, R. J., & Taylor, K. E. (2016). Overview of the Coupled Model Intercomparison Project Phase 6 (CMIP6) experimental design and organization. *Geoscientific Model Development*, *9*(5), 1937-1958. http://dx.doi.org/10.5194/gmd-9-1937-2016.

Franco, E. J. (2014). *Dimensionamento de bacias de detenção das águas pluviais com base no método racional* (Dissertação de mestrado). Universidade Federal do Paraná, Curitiba.

Hausfather, Z., & Peters, G. P. (2020). Emissions – the 'business as usual' story is misleading. *Nature*, *577*(7792), 618-620. PMid:31996825. http://dx.doi.org/10.1038/d41586-020-00177-3.

Ho, M., Lall, U., Allaire, M., Devineni, N., Kwon, H. H., Pal, I., Raff, D., & Wegner, D. (2017). The future role of dams in the United States of America. *Water Resources Research*, *53*(2), 982-998. http://dx.doi.org/10.1002/2016WR019905.

Kuo, C. C., & Gan, T. Y. (2015). Risk of exceeding extreme design storm events under possible impact of climate change. *Journal of Hydrologic Engineering*, *20*(12), 04015038. http://dx.doi.org/10.1061/(ASCE)HE.1943-5584.0001228.

Lee, B. S., & You, G. J. Y. (2013). An assessment of long-term overtopping risk and optimal termination time of dam under climate change. *Journal of Environmental Management*, *121*, 57-71. PMid:23524397. http://dx.doi.org/10.1016/j.jenvman.2013.02.025.

Lin, X., Huang, G., Piwowar, J. M., Zhou, X., & Zhai, Y. (2021). Risk of hydrological failure under the compound effects of instant flow and precipitation peaks under climate change: a case study of Mountain Island Dam, North Carolina. *Journal of Cleaner Production*, *284*, 125305. http://dx.doi.org/10.1016/j.jclepro.2020.125305.

Luna, R. M. (2000). *Utilização de técnicas de sensoriamento remoto e sistemas de informações geográficas em estudo de eventos de cheia*. Fortaleza: Universidade Federal do Ceará.

Mallakpour, I., AghaKouchak, A., & Sadegh, M. (2019). Climate-induced changes in the risk of hydrological failure of major dams in California. *Geophysical Research Letters*, *46*(4), 2130-2139. http://dx.doi.org/10.1029/2018GL081888.

Maurer, E. P., Kayser, G., Doyle, L., & Wood, A. W. (2018). Adjusting flood peak frequency changes to account for climate change impacts in the Western United States. *Journal of Water Resources Planning and Management*, *144*(3), 05017025. http://dx.doi.org/10.1061/(ASCE)WR.1943-5452.0000903.

Orlowsky, B., & Seneviratne, S. I. (2012). Global changes in extreme events: regional and seasonal dimension. *Climatic Change*, *110*(3–4), 669-696. http://dx.doi.org/10.1007/s10584-011-0122-9.

Ragno, E., AghaKouchak, A., Love, C. A., Cheng, L., Vahedifard, F., & Lima, C. H. R. (2018). Quantifying changes in future intensity-duration-frequency curves using multimodel ensemble simulations. *Water Resources Research*, *54*(3), 1751-1764. http://dx.doi.org/10.1002/2017WR021975.

Saboia, M. A. M., Souza Filho, F. A., Helfer, F., & Rolim, L. Z. R. (2020). Robust strategy for assessing the costs of urban drainage system designs under climate change scenarios. *Journal of Water Resources Planning and Management*, *146*(11), 05020022. http://dx.doi.org/10.1061/(ASCE)WR.1943-5452.0001281.

Schardong, A., Gaur, A., Simonovic, S. P., & Sandink, D. (2021). *Computerized tool for the development of intensity-duration-frequency curves under a changing climate: user's manual v.3* (Water Resources Research Report, No. 104, 80 p.). London: Facility for Intelligent Decision Support, Department of Civil and Environmental Engineering.

Silva, D. F., & Simonovic, S. P. (2020). *Development of non-stationary rainfall intensity duration frequency curves for future climate conditions* (Water Resources Research Report, No. 106, 49 p.). London: Facility for Intelligent Decision Support, Department of Civil and Environmental Engineering.

Simonovic, S. P., Schardong, A., & Sandink, D. (2017). Mapping extreme rainfall statistics for canada under climate change using updated intensity-duration-frequency curves. *Journal of Water Resources Planning and Management*, *143*(3), 04016078. http://dx.doi.org/10.1061/(ASCE)WR.1943-5452.0000725.

Srivastav, R. K., Schardong, A., & Simonovic, S. P. (2014). Equidistance quantile matching method for updating IDF curves under climate change. *Water Resources Management*, *28*(9), 2539-2562. http://dx.doi.org/10.1007/s11269-014-0626-y.

Tofiq, F. A., & Güven, A. (2015). Potential changes in inflow design flood under future climate projections for Darbandikhan Dam. *Journal of Hydrology*, *528*, 45-51. http://dx.doi.org/10.1016/j.jhydrol.2015.06.023.

Torrico, J. J. T. (1974). *Práticas hidrológicas*. Rio de Janeiro: Transcon. 120 p.

United States Department of Agriculture – USDA. (1986). *Urban hydrology for small watersheds* (Technical Release, No. 55). Washington: USDA.

Villela, S. M., & Mattos, A. (1975). *Hidrologia aplicada*. São Paulo: McGraw-Hill.

Vogel, R. M., Yaindl, C., & Walter, M. (2011). Nonstationarity: flood magnification and recurrence reduction factors in the United States. *Journal of the American Water Resources Association*, *47*(3), 464-474. http://dx.doi.org/10.1111/j.1752-1688.2011.00541.x.

Willems, P. (2013). Revision of urban drainage design rules after assessment of climate change impacts on precipitation extremes at Uccle, Belgium. *Journal of Hydrology*, *496*, 166-177. http://dx.doi.org/10.1016/j.jhydrol.2013.05.037.

Authors contributions

Brenda Lara Duarte Souza Carneiro: Methodology, Software, Formal analysis, Investigation, Data curation, Writing – original draft, Visualization.

Francisco de Assis de Souza Filho: Methodology, Conceptualization, writing – review & editing, supervision, project administration.

Taís Maria Nunes Carvalho: Formal analysis, writing – review & editing, supervision.

João Batista Sousa Raulino: Formal analysis, methodology, investigation.

Editor-in-Chief: Adilson Pinheiro

Associated Editor: Carlos Henrique Ribeiro Lima